Chapter 30
Application of a SANISAND Model for Numerical Simulations of the LEAP 2017 Experiments

Ming Yang, Andres R. Barrero, and Mahdi Taiebat

Abstract Numerical simulations of LEAP-UCD-2017 were performed to validate the numerical modeling approach and provide insight to capabilities and limitations of the adopted constitutive model. This chapter focuses on using an extended version of the SANISAND constitutive model implemented in *FLAC*^{3D} program at UBC. The constitutive model was calibrated based on the available laboratory element tests on Ottawa F65 sand. It was then used for simulation of the centrifuge tests on a mildly sloping liquefiable ground of the same soil subjected to dynamic loading. The study covered the Types B and C simulations and the sensitivity analyses. Type B simulations were successful in capturing some aspects of measurements from the experiments. A simplified approach for changing the soil permeability was adopted in Type C simulations, and the improved simulation results were again compared with those measured in the experiments. In the numerical sensitivity analyses, the model appeared to provide reasonable trends for simulation of different sample densities, and ground motion intensities and frequency contents.

30.1 Introduction

In geotechnical engineering, numerical modeling has become significantly more popular with the fast development of modeling tools and techniques. The key component of various continuum mechanics based numerical platforms for solving boundary value problems (BVP) is proper capturing of the material stress-strain response, or the material constitutive model. In recent decades, many advanced and sophisticated constitutive models have been developed, evaluated against laboratory element tests, and used in the analysis of dynamic problems related to soil liquefaction. Soil constitutive models are in a wide spectrum of sophistication. The developers often seek a balance between including sufficient features for capturing the key

M. Yang · A. R. Barrero · M. Taiebat (✉)
Department of Civil Engineering, University of British Columbia, Vancouver, BC, Canada
e-mail: mtaiebat@civil.ubc.ca

B. Kutter et al. (eds.), *Model Tests and Numerical Simulations of Liquefaction and Lateral Spreading*, https://doi.org/10.1007/978-3-030-22818-7_30

aspects of the mechanical response of soil and also keeping the models and, more importantly, their calibration sufficiently simple and straightforward, not an easy task particularly for a complex natural material like soil. The laboratory element tests are essential in the development of the constitutive models as they provide insight into the mechanical response of soil and can be used in evaluation of the range of applicability of the constitutive models. In the big picture, the goal of modeling in this field is the successful simulation of BVPs to provide an analysis-based insight for practical cases of interest in geotechnical engineering. As such, the experimental test on representative BVPs is also very essential in evaluation of the numerical modeling methods including (but not limited to) the role of the material constitutive models and their range of applicability and limitations. For geotechnical problems, centrifuge tests are particularly of interest in providing insights into the response of soil system BVPs. They have evolved and improved over the last three decades and can be sources of useful data for specific problems related to soil response subjected to dynamic loading. The Liquefaction Experiments and Analysis Project (LEAP) aims specifically at the combined use of advanced centrifuge testing and numerical modeling as described by Manzari et al. (2014).

The LEAP-UCD-2017 focused on evaluating the seismic response of a submerged, medium dense, clean sand with a mildly sloping surface subjected to base excitation. The exercise consisted of three phases. Phase 1 is on the constitutive model calibration based on the provided laboratory element tests on Ottawa F65 sand. Phase 2 is on the simulation of nine centrifuge experiments without knowing the experiment results; this is also referred to as Type B simulation. Phase 3 is re-evaluating the model simulation of the centrifuge experiments but now after knowing the centrifuge tests results; this is referred to as Type C simulation. In Type C simulations, the numerical modeling teams had the option to tune the constitutive model or the other simulation parameters or settings so as to achieve a closer match between the experiments and simulations. Along with Type C simulation settings, the simulation teams were requested to model another seven centrifuge tests without the corresponding experimental results provided, just to illustrate the simulation sensitivity to the key input parameters including the soil relative density, and the intensity and frequency content of the ground motion; this is referred to as sensitivity analysis.

This study focuses on explaining the numerical simulations conducted by the University of British Columbia (UBC) team for the LEAP-UCD-2017. It includes using an extended version of the SANISAND constitutive model following the simulation guidelines of the project. In Sect. 30.2, the constitutive model is briefly introduced and selected results of its calibration and performance are presented based on the available laboratory element tests on Ottawa F65 sand. Section 30.3 explains the key aspects of the finite difference model used for simulation of the LEAP centrifuge experiments. The results of Type B and Type C simulations and the sensitivity analyses on the selected input parameters are presented in Sect. 30.4. Brief conclusions and outlooks from the study are presented in Sect. 30.5.

30.2 Constitutive Model

This section includes a brief description of the constitutive model along with the calibration process and selected element test simulation results based on the available experimental data of cyclic triaxial and direct simple shear tests under undrained conditions on Ottawa F65 sand.

30.2.1 Extended SANISAND Model

The material constitutive model used by the UBC team for simulating both the element tests and the centrifuge tests in the LEAP-UCD-2017 is an extended version of the SANISAND model. The term SANISAND stands for Simple ANIsotropic SAND constitutive model. This class of sand constitutive models follows the elegant formulation of the original two-surface plasticity model developed by Manzari and Dafalias (1997). The model formulation is based on the bounding surface plasticity within the framework of critical state soil mechanics for unifying the description for different pressures and densities. The SANISAND class of models includes various extensions developed by Dafalias and Manzari (2004), Dafalias et al. (2004), Taiebat and Dafalias (2008), where the name SANISAND was first adopted, Li and Dafalias (2012) and Dafalias and Taiebat (2016). The work by Manzari and Dafalias (1997) represents the core of the constitutive model and the above-referenced subsequent works include various additional constitutive ingredients.

The version of SANISAND model with the fabric dilatancy effects by Dafalias and Manzari (2004), an overshooting correction scheme described in Dafalias and Taiebat (2016), and a work in progress extending the model formulation to capture the post-liquefaction response were considered as the constitutive model for this exercise. Inheriting 15 input parameters from the version of Dafalias and Manzari (2004), two overshooting correction parameters, and three post-liquefaction modeling parameters, this extended version includes 20 parameters as listed in Table 30.1 in detail. This model is focused on capturing stress-strain characteristics in the semi-fluidized regime during the liquefaction process. Its details are the subject of a forthcoming publication. This extended version is simply referred to as SANISAND hereafter. The model has been numerically implemented as a user-defined material model for application in the form of a dynamic link library (DLL) in the Finite Difference (FD) program *FLAC*^{3D} (Barrero 2019), which was used in the present study.

30.2.2 Calibration Process

In preparation for the Type B simulations, the SANISAND model was calibrated for simulation of a series of laboratory element tests on the designated Ottawa F65 sand

Table 30.1 Calibrated model parameters for SANISAND constitutive model

Parameter	Symbol	Value	Parameter	Symbol	Value
Elasticity	G_0	125	Kinematic	n^b	1.15
	ν	0.05	Hardening	h_0	5.0
Critical state line	M	1.26		c_h	0.968
	c	0.99	Fabric dilatancy	z_{max}	18
	e_0	0.78		c_z	500
	λ_c	0.029	Overshooting correction	e_{eq}^{-p}	0.01%
	ξ	0.7		n	1.0
Yield surface	m	0.02	Post-liquefaction	x_1	0.05
Dilatancy	n^d	1.25		x_2	50
	A_0	0.35		x_3	0.05

for the LEAP-UCD-2017. The experimental database includes a number of stress-controlled cyclic triaxial tests under undrained conditions, conducted and provided as part of the project to be used in the calibration process (El Ghoraiby et al. 2017, 2019). Besides, two additional sets of element test data on this type of sand were provided as supplementary data for the constitutive model calibration: monotonic and cyclic triaxial tests by Vasko (2015), and monotonic and cyclic direct simple shear tests by Bastidas (2016).

Details of the calibration process for the base model have been elaborated in the related reference as mentioned in Sect. 30.2.1, and also in Taiebat et al. (2010). The specific calibration of the model for the Ottawa F65 sand is presented in Ramirez et al. (2019) for all model parameters except for the last three that are related to the modeling of post-liquefaction. These latter parameters that are used for modeling the accumulation of post-liquefaction shear strains were approximated from the cyclic direct simple shear test data. Then the model parameters including c, n^b, h_0, n^d, A_0, c_z, z_{max} were slightly adjusted to better capture the stress-strain response of both the cyclic triaxial tests of the LEAP-UCD-2017 and the cyclic direct simple shear tests of Bastidas (2016). The final values of calibrated model parameters are listed in Table 30.1. The model performance for selected undrained cyclic triaxial tests at void ratios of 0.585 and 0.515 and also for selected undrained cyclic direct simple shear tests at void ratios of 0.802 and 0.539 are presented in Figs. 30.1 and 30.2, respectively.

30.3 Numerical Model Development

This section includes a brief introduction to the numerical modeling platform used in the present study. It follows by description of the model set up including the spatial discretization and mechanical and fluid boundary conditions, and simulation procedures related to initial condition set up, dynamic analysis parameters such as temporal discretization and numerical damping, and other provisions followed in the Type B and Type C simulations and the sensitivity analyses.

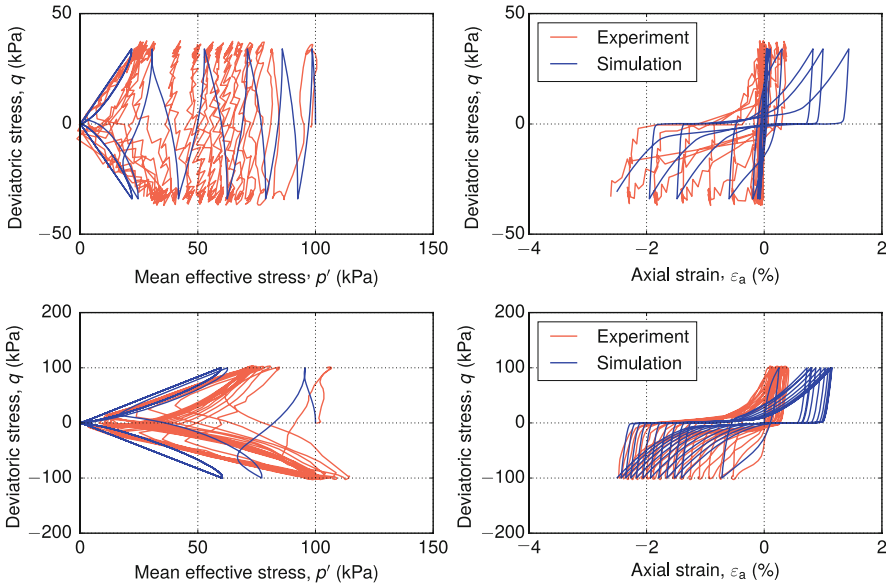

Fig. 30.1 Simulations versus experiments in stress-controlled cyclic triaxial tests on Ottawa F65 sand (El Ghoraiby et al. 2017, 2019) with initial void ratios 0.585 (top) and 0.515 (bottom)

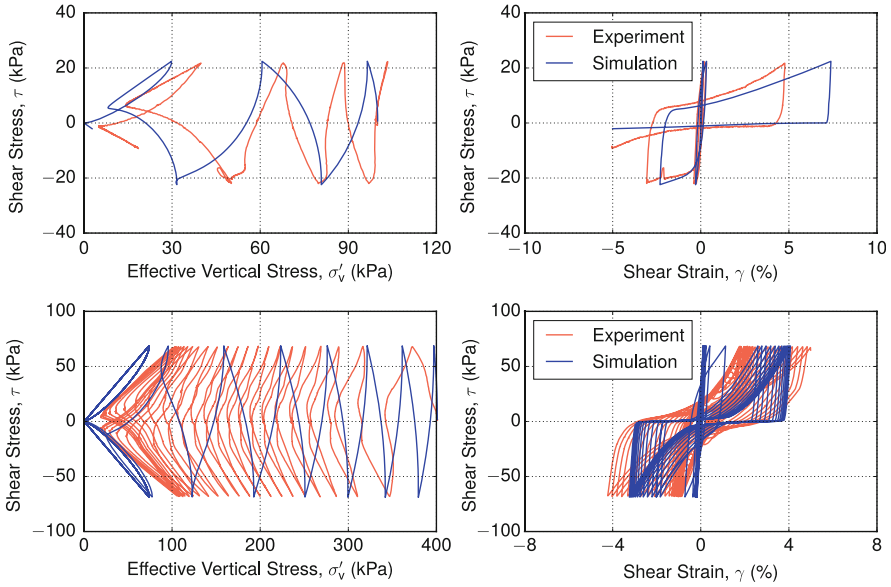

Fig. 30.2 Simulations versus experiments in cyclic direct simple shear tests on Ottawa F65 sand with initial void ratios 0.802 (top) and 0.539 (bottom); experimental data from Bastidas (2016)

30.3.1 General Numerical Platform

The analysis platform used in simulating centrifuge experiments is $FLAC^{3D}$ (Itasca Consulting Group 2013). $FLAC^{3D}$ is a three-dimensional explicit finite-difference program for engineering mechanics computation, extended from *FLAC* to simulate the behavior of three-dimensional structures built of soil, rock, and other materials that undergo plastic flow when their yield limits are reached. Materials are represented by polyhedral elements within a three-dimensional grid that is adjusted by the user to fit the shape of the object to be modeled. Each element behaves according to a prescribed linear or nonlinear stress/strain law in response to the applied boundary restraints.

This platform uses constant strain rate tetrahedral elements (sub-zones) that do not generate unwanted hour-glassing modes of deformation. When used in the framework of plasticity, these elements do not provide enough modes of deformation; e.g., they cannot deform individually without change of volume. To overcome this problem, a so-called mixed-discretization process is applied in $FLAC^{3D}$. In this procedure, the discretization for the isotropic part of stress and strain tensors are different from the discretization for the deviatoric part. The explicit Lagrangian calculation scheme and the mixed-discretization zoning technique used in $FLAC^{3D}$ are to ensure proper modeling of the plastic collapse and flow of the material. Each zone (hexahedron) in this program consists of two overlays of five sub-zones (tetrahedron), and in each sub-zone a constant strain rate is assumed. Thus, quantities such as displacements and pore pressures are accessible at the grid points while stresses and strains are only accessible at the sub-zone.

Two analysis configurations exist in $FLAC^{3D}$: fluid-mechanical interaction analysis and dynamic analysis. The formulation of coupled deformation–fluid diffusion processes in $FLAC^{3D}$ is done within the framework of the quasi-static Biot's theory and can be applied to problems involving single-phase Darcy flow in a porous medium. The dynamic analysis option extends the $FLAC^{3D}$ analysis capability to a wide range of dynamic problems in disciplines such as earthquake engineering, seismology, and mine rock bursts. The calculation is based on the explicit finite difference scheme to solve the full equations of motion using lumped grid point masses derived from the real density of surrounding zones. The dynamic feature can be coupled with the fluid-mechanical interaction feature, which makes $FLAC^{3D}$ capable of modeling dynamic pore pressure generation leading to liquefaction in cyclic loading process.

30.3.2 Numerical Model Description

A numerical model was prepared to represent the prototype scale of the centrifuge tests conducted in LEAP-UCD-2017. This included a three-dimensional finite difference mesh with only one zone along the slope strike direction to model all the centrifuge experiments. The mesh was not allowed to deform in the slope strike direction, and, therefore, worked in the same way as a plane strain condition. The mesh density, boundary conditions, and locations of the recording sensors/control

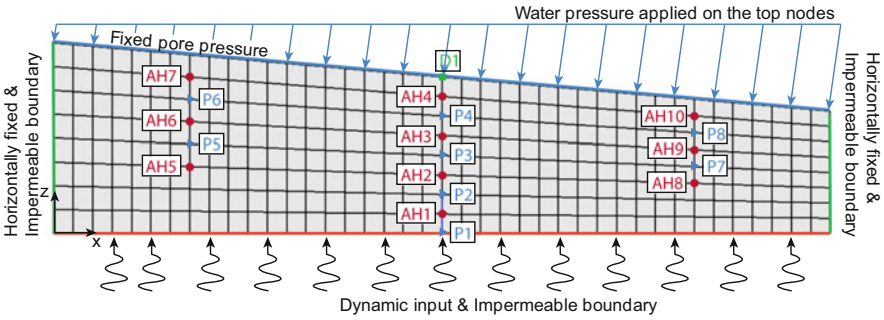

Fig. 30.3 Two-dimensional view of the *FLAC*^{3D} mesh showing the boundary conditions, and the recordings locations for the pore pressures (P), accelerations (AH), and displacements (D)

points are all presented in the two-dimensional view of the model geometry as shown in Fig. 30.3. In this figure AH1-AH10, P1-P8, and D1 refer to the acceleration, pore pressure, and displacement control points, respectively.

The mesh consists of 40 zones in the slope dip direction, 8 zones in the height direction, and 1 zone in the slope strike direction. The sizes of the zones are 0.5 m in the slope dip direction and 0.39–0.61 m in the height direction. In total, there are 320 zones and 738 grid points in this model. The grid points on the model base were fully constrained along all the three directions, while the grid points on the side walls were constrained laterally and the grid points on the top surface allowed full drainage with fixed values of pore pressure to model the submerged surface of the slope and replicated the situation in the centrifuge tests. After establishing the self-weight and the related initial conditions, the input motions were applied at the base grid points of the model for simulating the dynamic response of the slope, with the details presented in the following section.

30.3.3 Simulation Procedure

In order to establish a reasonable initial stress state of the model in the prototype scale, the numerical simulation started with stage construction of the slope where the dry soil deposit was constructed in layers and was allowed to establish the stress state under a gravity of 1*g*. In this process the mechanical boundary conditions are as shown in Fig. 30.3 except for the stress boundary condition on the top surface of the slope. A simple Mohr-Coulomb material model with bulk modulus 0.622 GPa, shear modulus 0.2385 GPa, and friction angle 33° was assigned to the sand layers to represent their stress-strain response. After the mechanical equilibrium was achieved for all layers of the slope deposit, the fluid-mechanical interaction was switched on, and a normal stress gradient representing the target submerged pressures of water was applied on the top surface of the slope, as shown in Fig. 30.3. The pore pressures

at the top surface were fixed to the submerged pressures of water during the analysis. When both mechanical and fluid equilibria were obtained, the sand constitutive model was switched to the elastoplastic model SANISAND with the target densities of the soil deposits for each centrifuge test. Once the constitutive model was adjusted to the new stress state, the dynamic analysis feature was utilized, and the processed acceleration records were applied at the base grid points of the slope. For Type B simulations, this processing included baseline correction and filtering of the high frequency content above 10 Hz. For Type C simulations and sensitivity analyses, the processing only included baseline correction. The simulation continued well beyond the end of the base excitation to dissipate excess pore pressure and allowed for the resulting settlement of the soil deposit.

FLAC^{3D} adopts the central finite difference approximation method for time integration, and for the simulations of the present study a mechanical ratio 10^{-6} was chosen as the convergence criterion in this process. In solid-fluid interaction, the water bulk modulus was chosen as 2.2×10^9 Pa, and the soil permeability was fixed to $k = 1.53 \times 10^{-4}$ m/s during the static stage of the analysis for establishing self-weight. In dynamic loading, a Rayleigh damping of 0.5% with the central frequency of 1 Hz was adopted. The soil permeability k was kept unchanged during the dynamic loading in Type B simulations. Following the suggestion of Shahir et al. (2012), the permeability can be argued to increase during the liquefaction state of material. To approximately account for that suggestion, the Type C simulations and sensitivity analyses were conducted using a time-dependent permeability that was increased to 10 k between $t = 6$ s and $t = 16$ s (an approximate time period representing the nearly liquefied state of the slope). It should be noted that the constitutive model parameters were kept the same for the Type B and Type C simulations and the sensitivity analyses.

30.4 Simulation Results

Results of the Type B and Type C numerical simulations are presented and compared with the experimental data for the nine centrifuge tests in terms of acceleration response spectra, excess pore pressures, and horizontal displacements at selected control points. Similar results are also reported from the numerical sensitivity analyses conducted on seven additional simulations that aim for variations of sand density and ground motion intensity and frequency content. Because of the limited space allowed for this chapter, a detailed description and analysis of the results will be presented in a more expanded forthcoming manuscript.

30.4.1 Type B and Type C Simulations

For the Type B simulations, the numerical modeling teams were provided with the information of laboratory element tests to be used for calibration of the constitutive

models, the configuration for the centrifuge tests, and the input motions. Based on this information, Type B simulations of the nine centrifuge tests (Madabhushi et al. 2019; Okamura and Nurani Sjafruddin 2019; Kim et al. 2019; Vargas Tapia et al. 2019; Hung and Liao 2019; Carey et al. 2019; Liu et al. 2019) were completed and the results for the accelerations pore pressures and horizontal displacements at the control points shown in Fig. 30.3 were reported. The corresponding experimental data were released after this stage. In Type C simulations, the simulation teams were allowed to adjust their parameters to get a better match to the centrifuge test results. The changes considered by this team in Type C simulations were limited to the use of variable permeability and not applying the high-frequency filter to the input motions, as described in the previous section.

The comparisons, at different control points, between the experimental recordings from the nine centrifuge tests and the corresponding Type B and Type C simulations are presented in this section. In the comparisons between the experiments and simulations, among the nine centrifuge tests, NCU3 is chosen to illustrate details of one centrifuge test at AH1-AH10 in the form of acceleration response spectra (Fig. 30.4) and at P1-P8 in the form of excess pore pressure time histories (Fig. 30.5). The simulation results match the experiments very well around the predominant

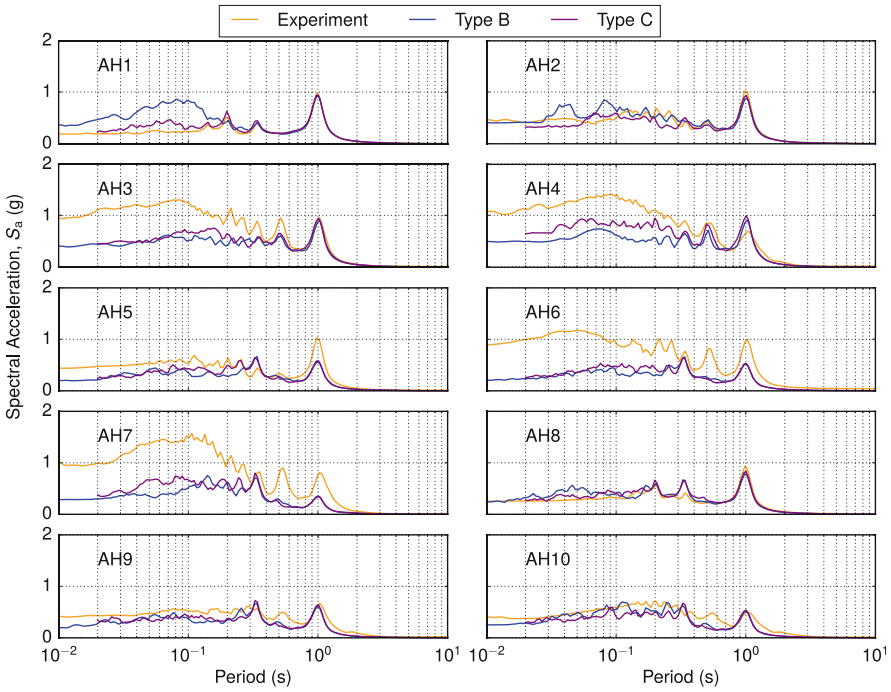

Fig. 30.4 Simulation results for the NCU3 centrifuge experiment: acceleration response spectra

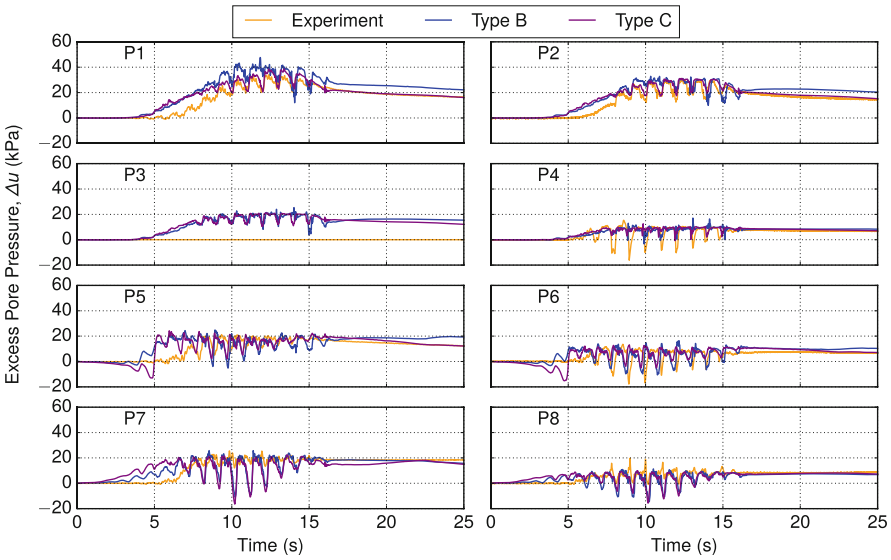

Fig. 30.5 Simulation results for the NCU3 centrifuge experiment: excess pore pressures

frequency of the input motion (1 Hz) except the accelerometers AH5, AH6, and AH7 located on the upslope side where the spectral accelerations are underestimated. Both experiments and simulations show presence of dilation pulses in the plots of excess pore pressure. The simulated dilation pulses in P7 appear to be stronger than those reported from the centrifuge test while in P4 the simulated ones appear to be weaker. Following this detailed comparisons of spectral acceleration and excess pore pressure in all control points of NCU3, results of all the other eight tests, but only at selected points, are presented to reveal the comparative performance of numerical models in simulating the centrifuge experiments. These results are presented only at AH1 (Fig. 30.6) and AH4 (Fig. 30.7) for accelerations, and P1 (Fig. 30.8) and P4 (Fig. 30.9) for excess pore pressures. Finally results of all nine tests for the horizontal displacement time histories at D1 are compared with the corresponding ones from the simulations (Fig. 30.10).

The results suggest that in most cases the comparisons between the experiments and simulations are reasonable for the acceleration response spectra and the excess pore pressure time histories. Simulation of the acceleration response spectra at higher frequencies and also the peak values of the excess pore pressure time histories appear to have improved in Type C simulations for a number of cases. While the simulations properly capture the trend of evolution of horizontal displacement at D1, in all cases the magnitude of simulated displacement appears to be larger or considerably larger than those derived from the experiments. Again the Type C simulations have improved the simulation of the displacements at D1.

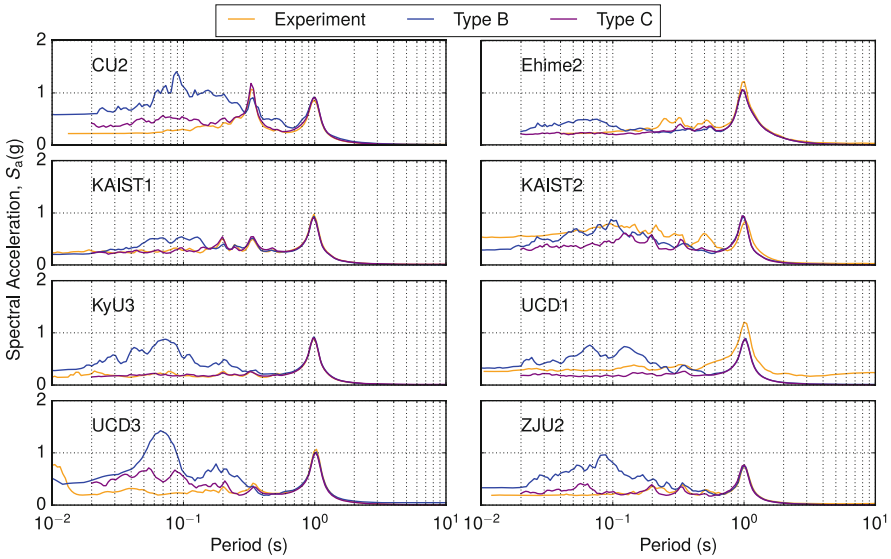

Fig. 30.6 Simulation results for the remaining eight centrifuge experiments: acceleration response spectra at AH1

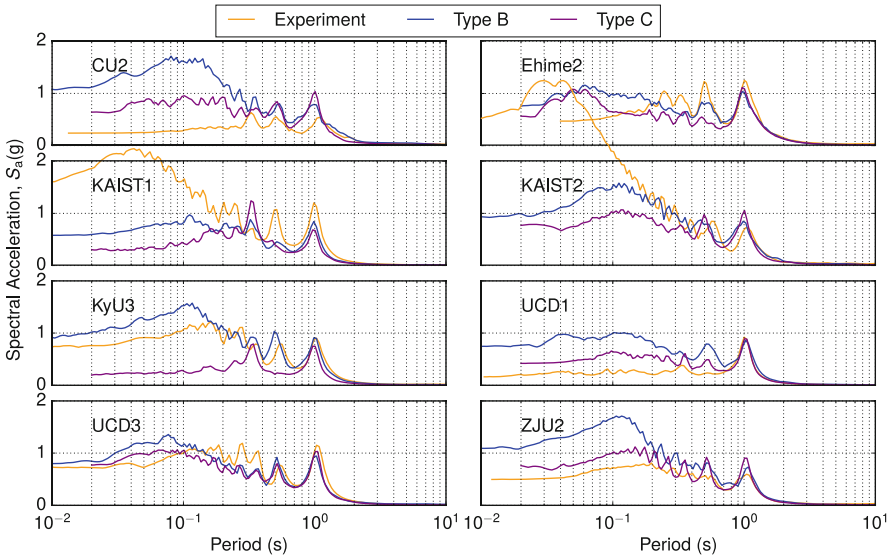

Fig. 30.7 Simulation results for the remaining eight centrifuge experiments: acceleration response spectra at AH4

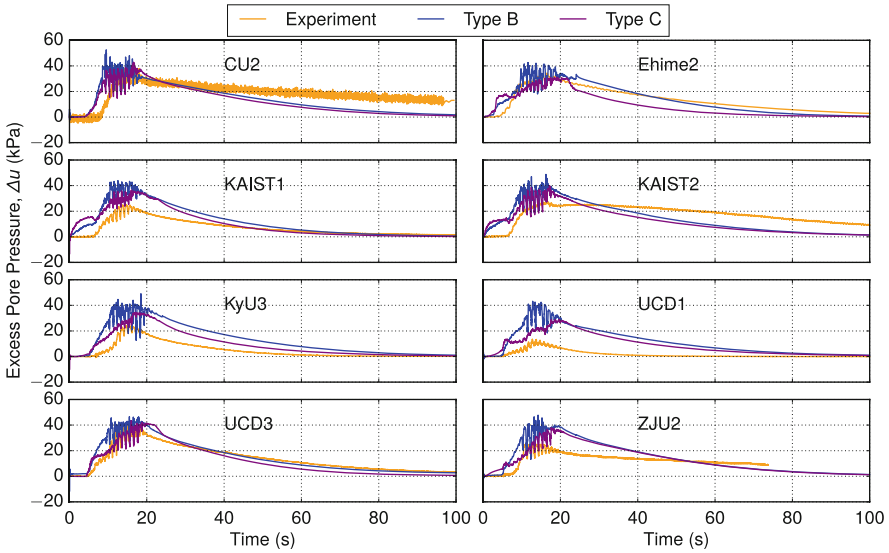

Fig. 30.8 Simulation results for the remaining eight centrifuge experiments: excess pore pressure at P1

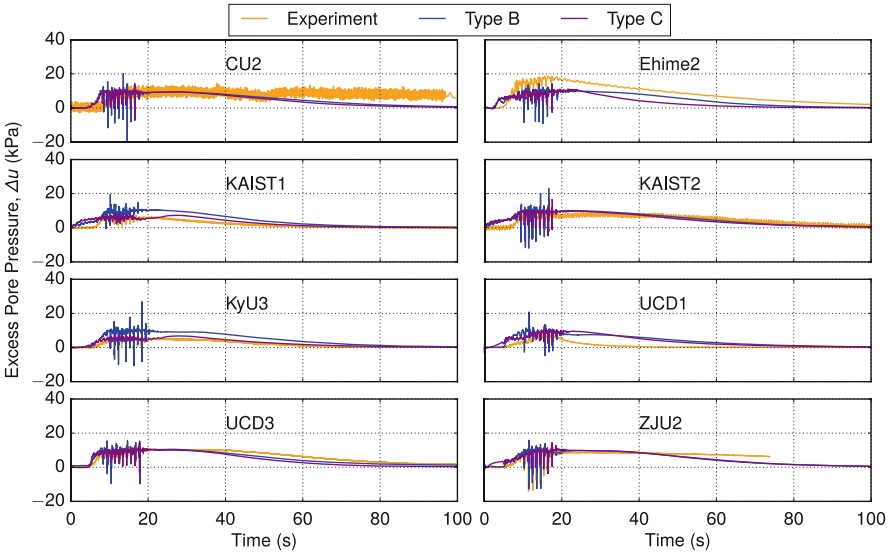

Fig. 30.9 Simulation results for the remaining eight centrifuge experiments: excess pore pressure at P4

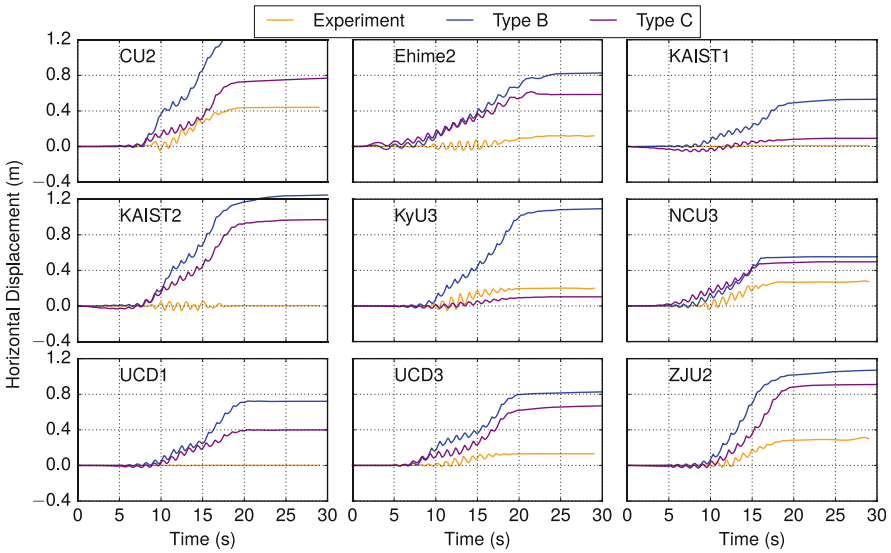

Fig. 30.10 Simulation results for all nine centrifuge experiments: horizontal displacements at D1

30.4.2 Sensitivity Analyses

With the same configurations as Type C simulations, numerical sensitivity analyses were also conducted on seven planned centrifuge tests, NS1-NS7, based on the provided densities of the sand layer and characteristics of the input motion, but the corresponding experimental results were not provided. In particular, these sensitivity analyses aim at variations of sand density (NS1, NS2, and NS3), ground motion intensity (NS1, NS4, and NS5), and frequency content (NS1, NS6, and NS7). Comparative simulation results at different control points are summarized in Figs. 30.11, 30.12, 30.13, and 30.14. The trends observed in the results appear to be reasonable and are illustrative of the features embedded in the constitutive model such as density dependency and small yield locus; the effects will be discussed and elaborated in details in a more extended manuscript.

30.5 Summary and Outlook

The extended version of SANISAND for the semi-fluidized regime of response is expected to have improved the predictive capabilities in capturing stress-strain loops beyond the onset of liquefaction. Several aspects of response in the centrifuge testing appear to have been captured by the numerical model. The lateral displacements, however, have been overpredicted in a number of cases. This is believed to be due to the performance of the calibrated model as can be observed also in the element level.

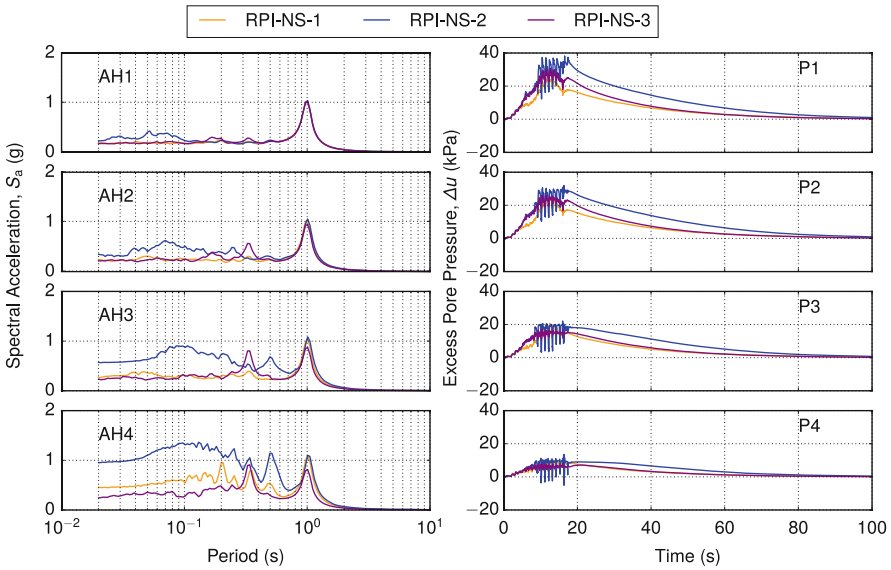

Fig. 30.11 Simulation results for sensitivity analysis on initial density: acceleration response spectra and excess pore pressures

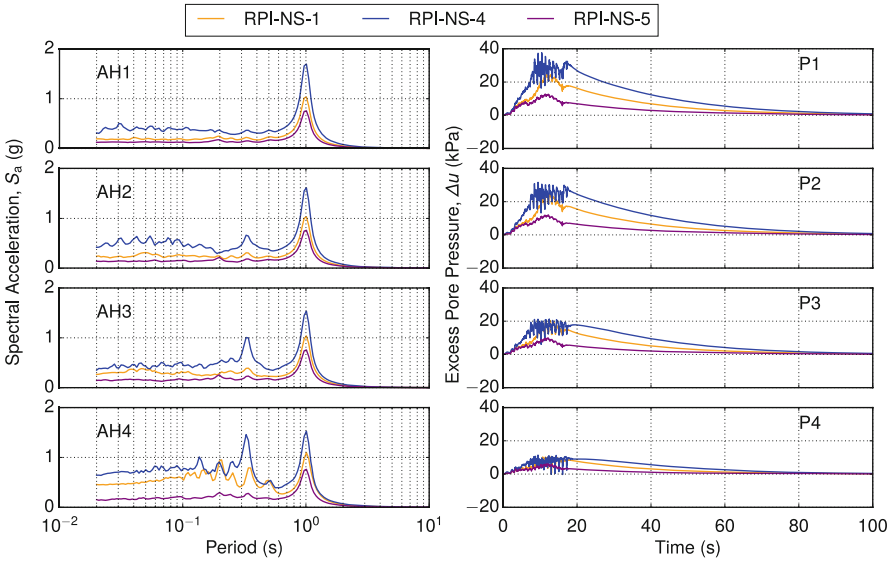

Fig. 30.12 Simulation results for sensitivity analysis on ground motion intensity: acceleration response spectra and excess pore pressures

A lower shear-induced volumetric stiffness in the pre-liquefaction stage, and a higher shear stiffness in the post-liquefaction stage are expected to improve the predictive capability of the model. The simulation results can be revisited by using such revised group of model parameters.

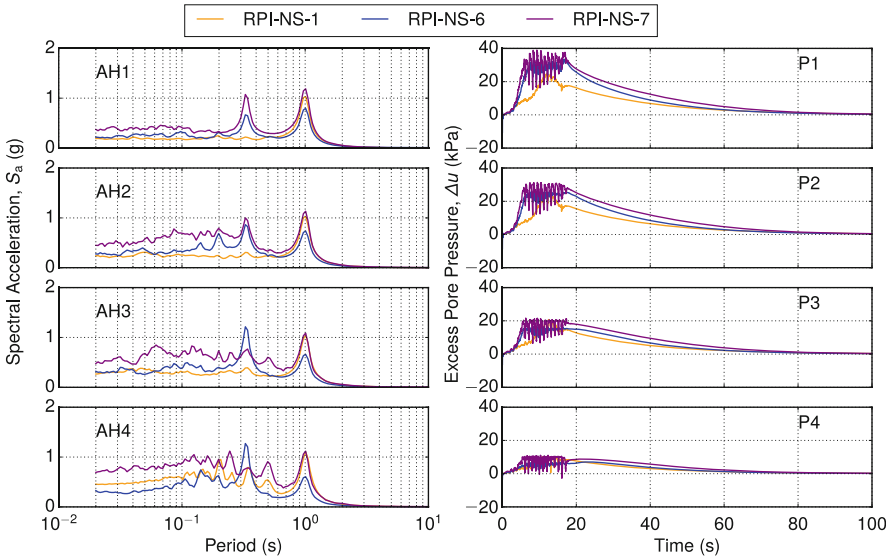

Fig. 30.13 Simulation results for sensitivity analysis on ground motion frequency content: acceleration response spectra and excess pore pressures

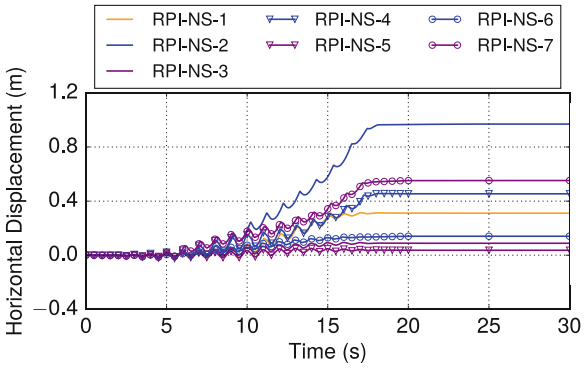

Fig. 30.14 Simulation results for sensitivity analysis: horizontal displacement at D1

References

Barrero, A. R. (2019). *Multi-Scale Modeling of the Response of Granular Soils Under Cyclic Shearing*. Ph.D. thesis, University of British Columbia (in preparation).

Bastidas, A. M. P. (2016). *Ottawa F-65 Sand Characterization*. Ph.D. thesis, University of California, Davis.

Carey, T. J., Stone, N., Hajialilue Bonab, M., & Kutter, B. L. (2019). LEAP-UCD-2017 centrifuge test at University of California, Davis. In B. Kutter et al. (Eds.), *Model tests and numerical simulations of liquefaction and lateral spreading: LEAP-UCD-2017*. New York: Springer.

Dafalias, Y. F., & Manzari, M. T. (2004). Simple plasticity sand model accounting for fabric change effects. *Journal of Engineering Mechanics, 130*(6), 622–634.

Dafalias, Y. F., Papadimitriou, A. G., & Li, X. S. (2004). Sand plasticity model accounting for inherent fabric anisotropy. *Journal of Engineering Mechanics, 130*(11), 1319–1333.

Dafalias, Y. F., & Taiebat, M. (2016). SANISAND-Z: Zero elastic range sand plasticity model. *Géotechnique, 66*(12), 999–1013.

El Ghoraiby, M. A., Park, H., & Manzari, M. T. (2017). *LEAP 2017: Soil Characterization and Element Tests for Ottawa F65 Sand*. Washington, DC: The George Washington University.

El Ghoraiby, M. A., Park, H., & Manzari, M. T. (2019). Physical and mechanical properties of Ottawa F65 sand. In B. Kutter et al. (Eds.), *Model tests and numerical simulations of liquefaction and lateral spreading: LEAP-UCD-2017*. New York: Springer.

Hung, W.-Y., & Liao, T.-W. (2019). LEAP-UCD-2017 centrifuge tests at NCU. In B. Kutter et al. (Eds.), *Model tests and numerical simulations of liquefaction and lateral spreading: LEAP-UCD-2017*. New York: Springer.

Itasca Consulting Group, Inc. (2013). *FLAC3D: Fast Lagrangian Analysis of Continua in 3 Dimensions, Ver. 5.01*. Minneapolis: Itasca.

Kim, S.-N., Ha, J.-G., Lee, M.-G., & Kim, D.-S. (2019). LEAP-UCD-2017 centrifuge test at KAIST. In B. Kutter et al. (Eds.), *Model tests and numerical simulations of liquefaction and lateral spreading: LEAP-UCD-2017*. New York: Springer.

Li, X. S., & Dafalias, Y. F. (2012). Anisotropic critical state theory: Role of fabric. *Journal of Engineering Mechanics, 138*(3), 263–275.

Liu, K., Zhou, Y.-G., She, Y., Peng Xia, D.-M., Huang, J.-S., Yao, G., & Chen, Y.-M. (2019). Specifications and results of centrifuge model test at Zhejiang University for LEAP-UCD-2017. In B. Kutter et al. (Eds.), *Model tests and numerical simulations of liquefaction and lateral spreading: LEAP-UCD-2017*. New York: Springer.

Madabhushi, S. S. C., Dobrisan, A., Beber, R., Haigh, S. K., & Madabhushi, S. P. G. (2019). LEAP-UCD-2017 centrifuge tests at Cambridge. In B. Kutter et al. (Eds.), *Model tests and numerical simulations of liquefaction and lateral spreading: LEAP-UCD-2017*. New York: Springer.

Manzari, M. T., & Dafalias, Y. F. (1997). A critical state two-surface plasticity model for sands. *Géotechnique, 47*(2), 255–272.

Manzari, M. T., Kutter, B. L., Zeghal, M., Iai, S., Tobita, T., Madabhushi, S. P. G., Haigh, S. K., Mejia, L., Gutierrez, D. A., Armstrong, R. J., Sharp, M. K., Chen, Y. M., & Zhou, Y. G. (2014). *LEAP projects: Concept and Challenges* (p. 109–116).

Okamura, M. & Nurani Sjafruddin, A. (2019). LEAP-2017 centrifuge test at Ehime University. In B. Kutter et al. (Eds.), *Model tests and numerical simulations of liquefaction and lateral spreading: LEAP-UCD-2017*. New York: Springer.

Ramirez, J., Barrero, A. R., Chen, L., Dashti, S., Ghofrani, A., Dafalias, Y. F., Taiebat, M., & Arduino, P. (2019). Site response in a layered liquefiable deposit: Evaluation of different numerical tools and methodologies with centrifuge experimental results. *ASCE Journal of Geotechnical and GeoEnvironmental Engineering, 144*, 10.

Shahir, H., Pak, A., Taiebat, M., & Jeremić, B. (2012). Evaluation of variation of permeability in liquefiable soil under earthquake loading. *Computers and Geotechnics, 40*, 74–88.

Taiebat, M., & Dafalias, Y. F. (2008). SANISAND: Simple anisotropic sand plasticity model. *International Journal for Numerical and Analytical Methods in Geomechanics, 32*, 915–948.

Taiebat, M., Jeremić, B., Dafalias, Y. F., Kaynia, A. M., & Cheng, Z. (2010). Propagation of seismic waves through liquefied soils. *Soil Dynamics and Earthquake Engineering, 30*(4), 236–257.

Vargas Tapia, R. R., Tobita, T., Ueda, K., & Yatsugi, H. (2019). LEAP-UCD-2017 centrifuge test at Kyoto University. In B. Kutter et al. (Eds.), *Model tests and numerical simulations of liquefaction and lateral spreading: LEAP-UCD-2017*. New York: Springer.

Vasko, A. (2015). *An investigation into the behavior of Ottawa sand through monotonic and cyclic shear tests*. Master thesis, The George Washington University.